Journal of Applied Polymer Science

Development and characterization of green composites from bio-based polyethylene and peanut shell

Daniel Garcia-Garcia,[1] Alfredo Carbonell-Verdu,[1] Amparo Jordá-Vilaplana,[2] Rafael Balart,[1] David Garcia-Sanoguera[1]

[1]Instituto De Tecnología De Materiales (ITM), Universitat Politècnica De València (UPV), Plaza Ferrandiz Y Carbonell 1, 03801, Alcoy, Alicante, Spain

[2]Departamento De Ingeniería Gráfica, Universitat Politècnica De València (UPV), Plaza Ferrandiz Y Carbonell 1, 03801, Alcoy, Alicante, Spain

Correspondence to: D. Garcia-Garcia (E-mail: dagarga4@epsa.upv.es)

ABSTRACT: In the present work, different compatibilizers, namely polyethylene-*graft*-maleic anhydride (PE-*g*-MA), polypropylene-*graft*-maleic anhydride (PP-*g*-MA), and polystyrene-*block*-poly(ethylene-*ran*-butylene)-block-polystyrene-*graft*-maleic anhydride (SEBS-*g*-MA) were used on green composites derived from biobased polyethylene and peanut shell (PNS) flour to improve particle–polymer interaction. Composites of high-density polyethylene/peanut shell powder (HDPE/PNS) with 10 wt % PNS flour were compatibilized with 3 wt % of the abovementioned compatibilizers. As per the results, PP-*g*-MA copolymer lead to best optimized properties as evidenced by mechanical characterization. In addition, best particle–matrix interface interactions with PP-*g*-MA were observed by scanning electron microscopy (SEM). Subsequently HDPE/PNS composites with varying PNS flour content in the 5–30 wt % range with PP-*g*-MA compatibilizer were obtained by melt extrusion and compounding followed by injection molding and were characterized by mechanical, thermal, and morphological techniques. The results showed that PNS powder, leads to an increase in mechanical resistant properties (mainly, flexural modulus, and strength) while a decrease in mechanical ductile properties, that is, elongation at break and impact absorbed energy is observed with increasing PNS flour content. Furthermore, PNS flour provides an increase in thermal stability due to the natural antioxidant properties of PNS. In particular, composites containing 30 wt % PNS powder present a flexural strength 24% and a flexural modulus 72% higher than the unfilled polyethylene and the thermo-oxidative onset degradation temperature is increased from 232 °C up to 254 °C thus indicating a marked thermal stabilization effect. Resultant composites can show a great deal of potential as base materials for wood plastic composites. © 2016 Wiley Periodicals, Inc. J. Appl. Polym. Sci. **2016**, *133*, 43940.

KEYWORDS: biopolymers and renewable polymers; compatibilization; composites; mechanical properties

Received 10 December 2015; accepted 19 May 2016
DOI: 10.1002/app.43940

INTRODUCTION

In recent years, increased awareness on environmental issues has been detected. This fact, together with the problems related to petroleum depletion has led to a breakthrough in the field of environmentally friendly materials development; much of this progress has been observed in the field of polymer composites, mainly on natural fiber reinforced plastics (NFRP) and wood plastic composites (WPC) for everyday applications.[1–4] The use of natural fillers into a polymeric matrix provides attracting advantages such as reduced costs, lightness, excellent balanced mechanical properties, etc., together with a marked low environmental impact.[5] Moreover, due to their aesthetic appearance (wood or natural product like) and the advantageous position against wood (low maintenance, high dimensional stability in wet conditions, and high resistance to biological attack), NFRPs and WPCs are increasingly used in sectors such as decoration, construction, and automotive.[3,6–9]

The main disadvantages of using natural fillers in a polymeric matrix is the relatively poor dispersion of the filler in the matrix and the low polymer–particle compatibility which leads to poor interface phenomena thus giving poor final properties. The highly hydrophobic polymeric matrix is not compatible with the highly hydrophilic filler (ligno-cellulosic material) which gives poor adhesion among matrix–filler interface and this is responsible for a decrease in mechanical and thermal performance of composites.[10–12] One of the methods used to enhance filler dispersion and polymer–filler adhesion/interaction is the use of compatibilizer agents such as maleic anhydride-grafted polypropylene (PP-*g*-MA) or maleic anhydride-grafted polyethylene (PE-*g*-MA).[5,10,12–17] These compatibilizers act as a bridge

between the ligno-cellulosic particle and the polymeric chains because of their dual functionality. Firstly, polyethylene or polypropylene fraction in PE-*g*-MA and PP-*g*-MA, respectively, can interact with some polymer chains due to chemical affinity while maleic anhydride groups in the compatibilizer structure can react with hydroxyl groups in ligno-cellulosic particle by an esterification reaction to give increased matrix–filler interactions which have a positive effect on particle dispersion and stiffness.[13,18] Despite this, ductile properties are not usually improved due to the brittleness that the filler provides because of presence of particle aggregates and matrix discontinuity, which promote stress concentration phenomena.

Peanut is one of the most important crops in the world. Its world production is estimated around 30 million tons per year and most of it, is sold without the shell, which contributes to a high waste generation coming from the shell. A small amount of these wastes is used as animal feeding or valued by incineration.[19] Nevertheless, the greater part is disposed of in landfills with the subsequent high environmental impact. Peanut shell (PNS) is composed of natural polymers, mainly consisting in cellulose, lignin, hemicelluloses, and tannins.[20] Its chemical composition is similar to that of hard wood but PNS possesses higher cellulose content.[21] This feature makes PNS an interesting candidate as ligno-cellulosic filler in polymeric matrices. Up to now there are not many works focused on the use of PNS as filler in polymer matrices. Sareena *et al.*[22] evaluated the mechanical properties of composite materials based on a natural rubber matrix with PNS fillers. The study was focused on the effect of the particle size and the previous alkaline treatment on final performance of composites. Wu,[23] studied the effect of PNS reinforcements on mechanical and biodegradation properties of poly(butylene adipate-*co*-terephthalate)-PBAT composites. This work also evidenced the synergistic effect of PBAT-based compatibilizers (PBAT-*g*-MA) on final performance of PBAT-based composites. Salasinska *et al.*[24] investigated the effect of PNS load on mechanical and thermal behavior of high density polyethylene (HDPE) films. Zaaba *et al.*[25] showed the positive effect of previous chemical modification of PNS with poly(vinyl alcohol)-PVA to improve overall properties of recycled polypropylene (PP). Prabhakar *et al.*[26] analyzed the effect of PNS fillers (without and with a previous alkaline treatment) in epoxy thermosetting resins. In addition, the potential of PNS as base material for particle board manufacturing was studied,[27,28] but its use is not generalized. By taking into account the large amounts of PNS wastes and considering the increasing concern about environment and sustainable development, new materials are being demanded by our society to give an environmentally friendly solution to wastes. This has led to an increase in research about thermoplastic composites with natural fillers such as NFRPs and WPCs which use commodity, recycled or biodegradable plastics as matrices. Nevertheless, most of these studies are focused on the use of wastes coming from the wood industry.[29–31]

One pioneer company in the development of biobased polyolefins is Braskem. This company produces at commercial scale a biobased polyethylene from bioethanol derived from sugarcane but with similar properties to those of conventional petroleum-based polyethylene; nevertheless the environmental efficiency is considerably higher as 1 ton of the so called "green-PE" fixes 2.5 ton CO_2 thus having a positive overall effect on environment and the carbon footprint.[32]

The main goal of this work is to obtain high environmentally friendly biobased composites by using biobased HDPE as matrix and PNS waste from the food industry. The effect of different compatibilizers and filler content is shown. In the first part of the study, the effect of 3 wt % of different maleic anhydride-based copolymers is evaluated. Several studies in the literature suggest that this compatibilizer content can lead to optimum results in polymer composites with lignocellulosic fillers.[33–35] In particular, the effect of polyethylene-*graft*-maleic anhydride (PE-*g*-MA), polypropylene-*graft*-maleic anhydride (PP-*g*-MA) and polystyrene-*block*-poly(ethylene-*ran*-butylene)-block-polystyrene-graft-maleic anhydride (SEBS-*g*-MA) is evaluated in terms of mechanical properties and particle–polymer interaction. Once the best compatibilizer is selected, the PNS powder content is varied in the 5–30 wt % to investigate the effect of the filler loading on overall properties on compatibilized formulations. Mechanical properties are obtained by tensile, flexural, impact, and hardness tests. Thermo-oxidative degradation is studied by differential scanning calorimetry (DSC). Thermo-mechanical behavior is assessed by following the evolution of the storage modulus, G' and damping factor, tan δ. Degradation at high temperatures is evaluated by thermogravimetric analysis (TGA) and finally, particle–polymer interaction is observed by scanning electron microscopy (SEM).

EXPERIMENTAL

Materials

The polymer matrix was a commercial biobased HDPE grade Green HDPE SHA7260 supplied by Braskem (BRASKEM, Sao Paulo, Brazil). This is obtained from bioethanol derived from sugarcane and its minimum biobased content is 94% according to ASTM D6866 as indicated in the technical datasheet. This polyethylene has a density of 0.955 g/cm^3 and a melt flow index of 20 g/10 min measured at 190 °C.

The selected lignocellulosic filler was PNS from local food industry. Prior to composite manufacturing the PNS was subjected to a dry milling process in an ultra-centrifugal mill (Retsch GmbH, Hann, Germany) working at 8000 rpm, equipped with a 250 μm sieve; after the milling–sieving process, the obtained powder was subjected to a drying process at 80 °C for 4 h to remove residual moisture. The antioxidant capacity of PNS powder was determined by two different methods: DPPH and FRAP methods and the polyphenol and flavonoid total content was measured by the Folin–Ciocalteu method. Table I summarizes the main properties of PNS powder.

All three compatibilizer copolymers were supplied by Sigma Aldrich (Sigma Aldrich, Madrid, Spain) and were used to increase particle–polymer interactions and promote filler dispersion. These copolymers were polyethylene-*graft*-maleic anhydride (PE-*g*-MA), polypropylene-*graft*-maleic anhydride (PP-*g*-MA) and polystyrene-*block*-poly (ethylene-*ran*-butylene)-block-polystyrene-*graft*-maleic anhydride (SEBS-*g*-MA). Table II shows the main characteristics of these compatibilizers.

Table I. Characterization of the Antioxidant Capacity and Polyphenol and Flavonoid Total Content of PNS Powder

Property	Value
Antioxidant capacity, DPPH (%RSA)	83 ± 2
Antioxidant capacity, FRAP (mg Trolox/g sample)	1.33 ± 0.05
Flavonoids (mg quercentin/g sample)	1.16 ± 0.06
Polyphenols FOLIN (mg quercentin/g sample)	6.16 ± 0.27

HDPE/PNS Composite Manufacturing

In a first stage, four different composites were manufactured with HDPE and PNS powder (PNS). The PNS content was 10 wt % for all four composites and 3 wt % of different compatibilizers was added. Table III summarizes the compositions used to evaluate the influence of the compatibilizer type.

After selecting the most suitable compatibilizer for HDPE/PNS composites, new formulations containing 5, 10, 20, and 30 wt % PNS powder were manufactured.

All composites were obtained by following this procedure: polyethylene pellet, PNS powder and the corresponding amounts of compatibilizer were mechanically mixed in a zipper bag to homogenize and then fed into a twin screw co-rotating extruder with $D = 25$ mm and $L/D = 24$ from DUPRA S.L. (Alicante, Spain). The temperature profile was set to 160 °C, 160 °C, 165 °C, and 170 °C (from hopper to die). After cooling at room temperature, the obtained compounds were pelletized in a mill and subsequently processed by injection molding in a Meteor 270/75 (Mateu & Solé, Barcelona, Spain) at an injection temperature profile of 160 °C (hopper), 160 °C, 165 °C, 170 °C, and 170 °C (die). The filling time was 1 s and the cooling time was set to 10 s. After injection molding, standard samples for tensile tests (type 1B) as recommended by ISO 527 were obtained. Samples for tensile tests sized 150 mm in length, 4 mm thickness, and 10 mm wide. In addition, rectangular samples sizing 80 × 10 × 4 mm^3 were obtained for further characterization.

Mechanical Characterization of HDPE/PNS Composites

Tensile and flexural properties of HDPE/PNS composites were tested in a universal test machine Ibertest ELIB 30 (S.A.E. Ibertest, Madrid, Spain) at room temperature, according to ISO 527-5 and ISO 178, respectively, with a load cell of 5 kN and a crosshead rate of 5 mm/min. A minimum of five different samples were tested and average values were calculated.

With regard to hardness, a Shore D durometer 673-D (Instrumentos J. Bot S.A., Barcelona, Spain) was used according to the guidelines of the UNE-EN-ISO 868 standard. Charpy impact tests were carried out in a 1 J Charpy pendulum (Metrotec S.A., San Sebastián, Spain) as indicated by the ISO 179:1993. Five different notched samples values were averaged. The notch was "V" type at 45° and notch radio of 0.25 mm.

Table II. Summary of the Main Characteristics of Maleic Anhydride-Based Compatibilizers: PP-*g*-MA, PE-*g*-MA, and SEBS-*g*-MA

Properties	PP-*g*-MA	PE-*g*-MA	SEBS-*g*-MA
Maleic anhydride content (wt %)	8–10	~0.5	~2
Density at 25 °C (g/mL)	0.934	0.92	0.91

Table III. Summary of Compositions and Codes of Biobased HDPE/PNS Powder Formulations Used to Evaluate the Influence of the Compatibilizer Type on Overall Properties of Composites

Code	wt % green-PE	wt % PNS powder	wt % compatibilizer
HDPE/PNS	90	10	—
HDPE/PNS/PE-*g*-MA	87	10	3 [PE-*g*-MA]
HDPE/PNS/PP-*g*-MA	87	10	3 [PP-*g*-MA]
HDPE/PNS/SEBS-*g*-MA	87	10	3 [SEBS-*g*-MA]

In addition, dynamic mechanical thermal analysis (DMTA) was carried out in an oscillatory rheometer AR G2 (TA Instruments, New Castle) equipped with a torsion clamp for solid samples. Rectangular samples sizing 40 × 10 × 4 mm^3 were subjected to a temperature sweep from −50 °C up to 100 °C at a heating rate of 2 °C/min. Samples were tested at a frequency of 1 Hz and a percentage deformation (γ) of 0.1%.

SEM Characterization of Fractured Surfaces of HDPE/PNS Composites

A SEM Phenom (FEI Company, Eindhoven, The Netherlands) operated at 5 kV and an emission current of 50 μA was used to analyze the fractured surfaces from impact tests. In a previous stage, samples were metallized with a gold-palladium alloy in vacuum conditions in a sputter coater EMITECH mod. SC7620 (Quorum Technologies Ltd., East Sussex, UK).

Thermal Analysis of HDPE/PNS Composites

Thermal properties of neat HDPE, PNS powder and different HDPE/PNS composites were evaluated by DSC and TGA. TGA tests were carried out in a TGA/SDTA 851 thermobalance (Mettler-Toledo Inc., Schwerzenbach, Switzerland) with a heating program from 30 °C up to 700 °C at a heating rate of 20 °C/min in nitrogen atmosphere (with a constant flow rate of 66 mL/min). Thermal transitions were studied by differential scanning calorimetry in a DSC Mettler-Toledo 821 (Mettler-Toledo Inc., Schwerzenbach, Switzerland). Samples with average weight of 10 mg were subjected to a heating program from 30 to 300 °C at a heating rate of 10 °C/min in air atmosphere to evaluate the effect of natural phenolic compounds and flavonoids on thermal stabilization.

Water Uptake of HDPE/PNS Composites

Water uptake was assessed by immersion of samples in distilled water at room temperature. Three different samples of each composite formulations (80 × 10 × 4 mm^3) were subjected to water uptake and average values were calculated. Before starting the tests, samples were dried at 80 °C for 4 h to remove residual moisture. Weight changes were measured every 3 days for a total period of 7 months. The percentage water uptake was calculated by using eq. (1):

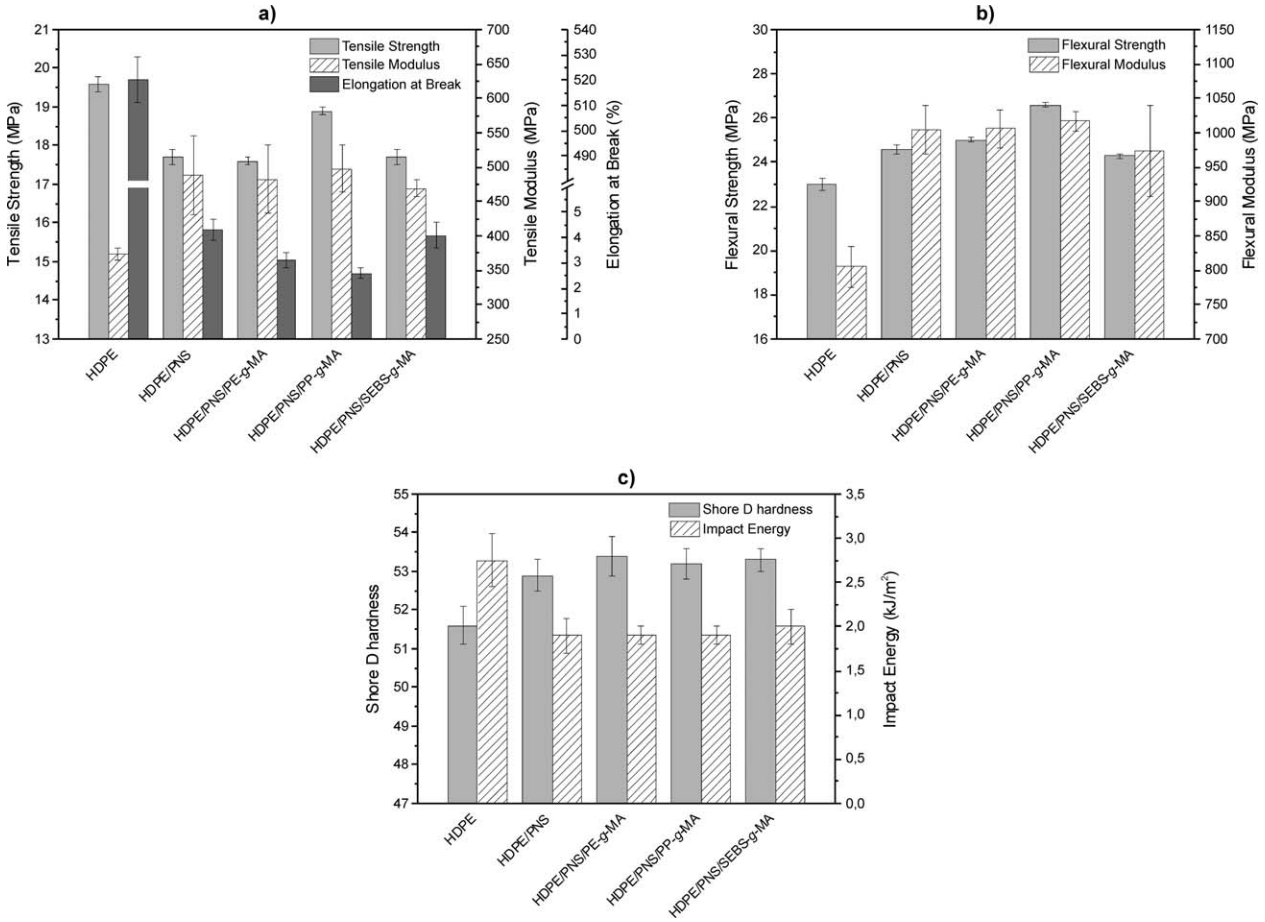

Figure 1. Bar plot with the evolution of (a) tensile properties, (b) flexural properties, and (c) Shore D hardness-impact energy of HDPE/PNS composites without and with different maleic anhydride based compatibilizers.

$$\text{Water uptake } (\%) = \frac{(M_f - M_i)}{M_i} \times 100 \qquad (1)$$

where, M_f is the final weight of the sample at a particular time and M_i is the initial weight of the dry sample before immersion in water.

RESULTS AND DISCUSSION

Effect of Different Maleic Anhydride-Based Copolymers as Compatibilizers for HDPE/PNS Composites

Figure 1 gathers the information about mechanical properties of HDPE/PNS composites (tensile, flexural, impact, and hardness) without and with different compatibilizers based on maleic anhydride modification.

With regard to tensile properties [Figure 1(a)], a slight decrease in tensile strength can be observed when PNS powder is added. Best results for tensile strength are obtained by using PP-*g*-MA (HDPE/PNS/PP-*g*-MA) that contributes to a tensile strength of 18.9 MPa which represents a percentage decrease of about 3% with regard to unfilled polyethylene (19.6 MPa). Tensile modulus is similar for all composites with values in the 400–500 MPa range, which is slightly higher in comparison to unfilled HDPE with a tensile modulus of about 373 MPa. In general, the tensile resistant properties are not remarkably influenced by the addition of 10 wt % PNS powder. Nevertheless, the elongation at break (ductile mechanical property) is reduced in a remarkable way as in most NFRP and WPC. The initial elongation at break of unfilled HDPE is around 520% and this value decreases dramatically up to values in the 2–4% range. This is due to presence of PNS particles dispersed in the polymeric matrix. The highly hydrophilic nature of PNS powder (lignocellulosic) is not compatible with the highly hydrophobic polyethylene matrix. This fact leads to a lack of particle–filler interactions which, in turn, has a key role in stress concentration phenomena.[36] Moreover, particle aggregates also contribute to stress concentration with a negative effect on cohesive properties such as elongation at break. Although slightly higher elongation at break is obtained for uncompatibilized HDPE/PNS composite, in general, the decrease in elongation at break is dramatic for all compositions with and without compatibilizer agents. It is evident that most of the elongation is lost with relatively low lignocellulosic filler content and this can restrict some final uses of HDPE/PNS composites (mainly in those that require high elongation ability). The main advantage of these composites is related to aesthetics concerns as they emulate wood like materials. Some engineering applications require high stiffness materials while no high elongation levels are needed as it is the case of furniture, decking, flooring, etc. So that, alternative uses to HDPE can be derived with addition of PNS flour.

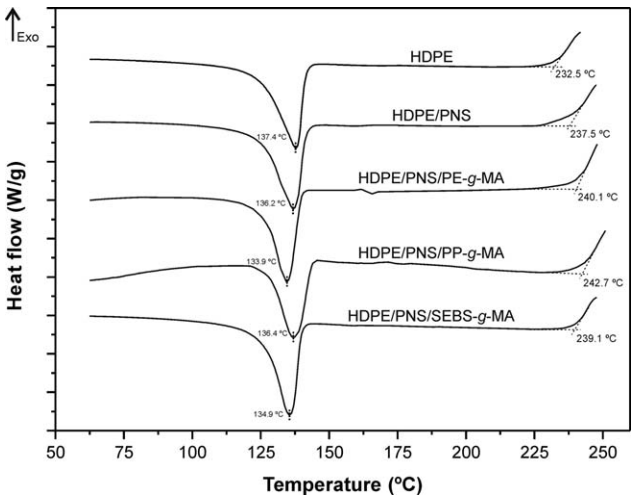

Figure 2. Comparative plot of calorimetric (DSC) curves of neat HDPE and HDPE/PNS composites with different compatibilizer agents.

With regard to flexural properties [Figure 1(b)], once again it is the HDPE/PNS/PP-*g*-MA composite the one that offers the highest flexural strength (26.6 MPa) which represents a % increase of about 16% with regard to unfilled HDPE (23 MPa) and 8% more than uncompatibilized HDPE/PNS composite. Identical tendency can be observed for the flexural modulus with values of 1017 MPa for composites compatibilized with PP-*g*-MA which represents a % increase of almost 26% with regard to the unfilled HDPE.

Impact energy [Figure 1(c)] is another mechanical property highly sensitive to presence of stress concentrators. All composites show absorbed energy values close to 2 kJ/m^2 which represents a % decrease of about 27% if compared with the unfilled material (2.75 kJ/m^2). Impact energy indicates the absorbed energy during deformation and fracture processes. This depends on several factors such as stress concentrators, crack formation and growth rate, filler particle size, etc. All these phenomena are involved in the overall deformation and, consequently, can affect the impact-absorbed energy. As we have seen before, the tensile strength is slightly lower and the flexural strength increases; nevertheless, the addition of PNS powder restricts in a remarkable way the ability of HDPE/PNS composites to deform so that, the overall effect is a small decrease in absorbed energy.

With regard to Shore D hardness [Figure 1(c)], as it is a resistant mechanical property, a slight increase can be observed but no remarkable differences with the compatibilizer type can be distinguished.

Thermal behavior of HDPE/PNS has been evaluated with DSC and TGA. Thermo-oxidative degradation at moderate temperatures in the processing window was studied by DSC whilst thermal degradation–decomposition at high temperatures was followed by TGA. Figure 2 shows the melt temperature (peak) and the onset degradation (thermo-oxidative processes) temperature for unfilled and HDPE/PNS composites. Thermo-oxidative processes at moderate temperatures are related to free radical formation due to chain scission and subsequent reaction with oxygen moieties, but no detectable weight loss is observed at this stage. For this reason, thermo-oxidative processes are best detected by DSC. As we can see, the melt temperature for HDPE/PNS composites is slightly lower, probably due to nucleating effect of lignocellulosic particles but the overall effect is negligible. Nevertheless, it is important to remark a noticeable delay in the thermo-oxidative processes at moderate temperatures in the typical processing temperature range for all uncompatibilized and compatibilized HDPE/PNS composites. This delay leads to broaden the processing window of HDPE/PNS composites. The uncompatibilized HDPE/PNS composite shows an onset thermo-oxidation temperature of 237.5 °C which is 5 °C higher than the unfilled HDPE (232.5 °C). All compatibilized HDPE/PNS composites offer slightly higher onset thermo-oxidation temperatures close to 240 °C but it is the use of PP-*g*-MA compatibilizer (HDPE/PNS/PP-*g*-MA) the one that gives the optimum results. This increase in the onset thermo-oxidation temperature is directly related to the presence of phenolic compounds and flavonoids with high free-radical scavenging activity as described previously.

Degradation at high temperatures (beyond the thermo-oxidation temperature range) was studied by TGA. Figure 3 shows TGA curves of HDPE/PNS composites together with TGA curves for raw materials. As it can be seen in the TGA curve for neat HDPE, no weight loss is detected in the temperature range of the thermo-oxidative process observed by DSC. For this reason, thermo-oxidative process was followed by DSC and degradation at high temperatures with the corresponding weight loss was studied by TGA. As it can be observed, degradation of PNS powder occurs in four different stages. The first one, with a weight loss of about 5%, is located between 50 and 150 °C and corresponds to residual moisture evaporation.[27] The second stage takes place in the 220–350 °C range with a weight loss of 40% which corresponds to decomposition of low molecular weight components such as hemicelluloses and glycosidic bonds in cellulose. The third stage, characterized by a weight loss of 14%, occurs between 350 and 410 °C and is directly related to thermal decomposition of cellulose. Finally, above

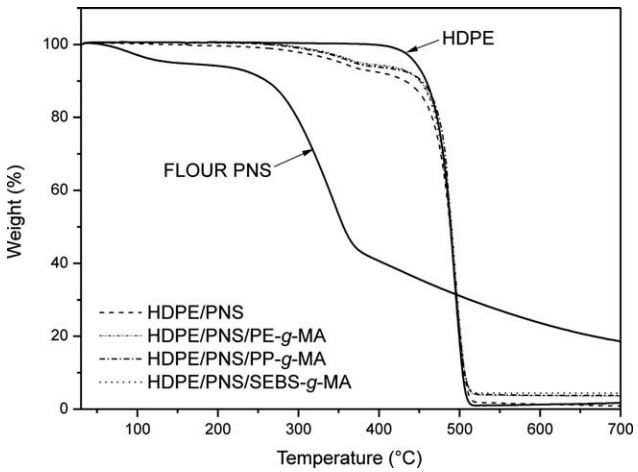

Figure 3. Comparative plot of the thermogravimetric (TGA) curves of neat HDPE, peanut shell powder (PNS) and HDPE/PNS composites with different compatibilizer agents.

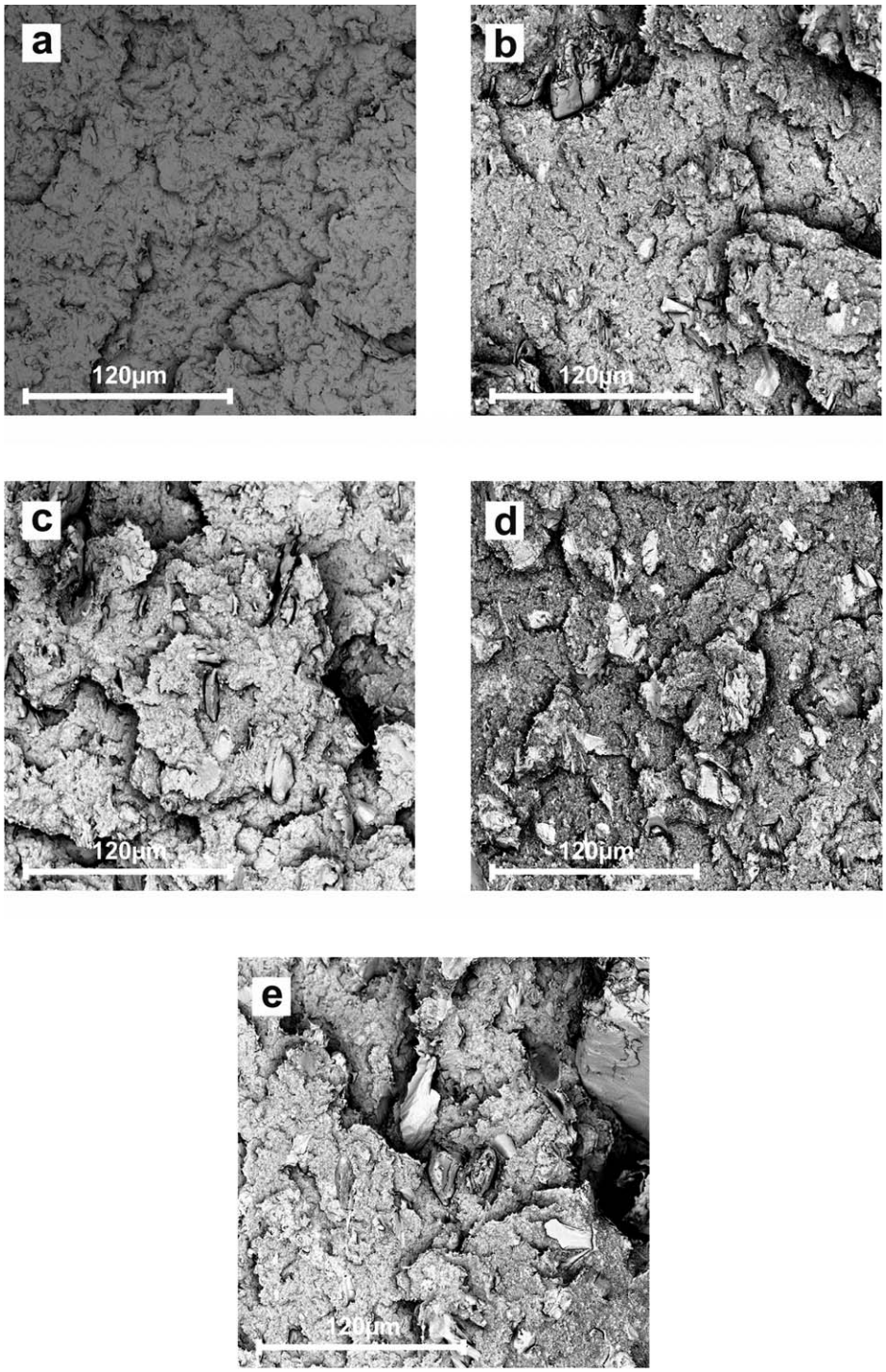

Figure 4. SEM images from fractured surfaces (1000×) of neat HDPE and HDPE/PNS with different compatibilization systems (a) HDPE, (b) HDPE/PNS, (c) HDPE/PNS/PE-*g*-MA, (d) HDPE/PNS/PP-*g*-MA, and (e) HDPE/PNS/SEBS-*g*-MA.

410 °C lignin degradation occurs.[5,37] It is worth to notice that lignin degradation starts prior to other components but the degradation rate is slower.[38] With regard to raw HDPE, degradation proceeds in a one step process that starts at about 350 °C and ends around 520 °C with a weight loss of almost 99% (very low char generation).[39] To evaluate the degradation process of HDPE/PNS composites it is important to consider that some processes can be overlapped. HDPE is a highly hydrophobic polymer so that, no weight loss is observed in the temperature range comprised between 50 and 150 °C related to moisture removal and the typical degradation range for hemicelluloses (220–350 °C) is lower than the onset decomposition temperature for HDPE. As it can be observed, HDPE decomposition overlaps with the cellulose and lignin degradation in the 350–

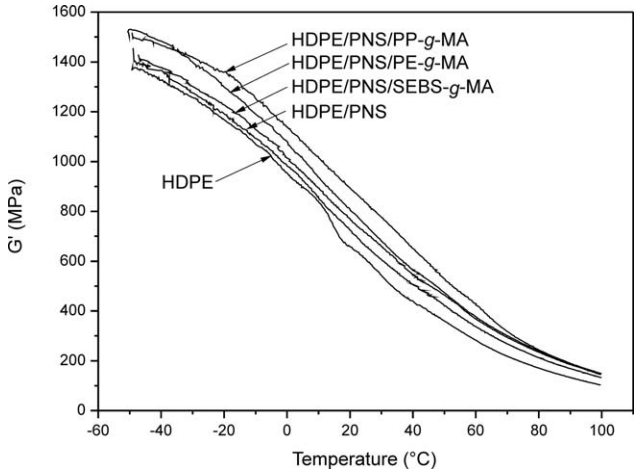

Figure 5. Evolution of the storage modulus (G') of HDPE/PNS composites (10 wt % PNS) with and without different compatibilizer agents.

520 °C range. Decomposition of HDPE/PNS composites with and without compatibilizers show a combination of the two previously described behaviors. Presence of PNS powder in HDPE/PNS composites leads to a decrease in thermal stability at high temperatures and two different stages can be clearly identified. The first one occurs between 230 and 420 °C and corresponds to degradation of hemicelluloses, cellulose and lignin from PNS powder. Above 420 °C, degradation of HDPE chains occur.[10] As we have previously observed, PNS powder degradation forms important amounts of char after combustion so that, residual char is also detectable for HDPE/PNS composites. It is also possible to observe that the overall effect of compatibilizers is positive as slightly better thermal stability is obtained compared with uncompatibilized HDPE/PNS. This fact is probably due to particle-matrix interactions as some hydroxyl groups in PNS powder particles (mainly from cellulose and hemicelluloses) are esterified with anhydride groups in the different compatibilizer agents.[10]

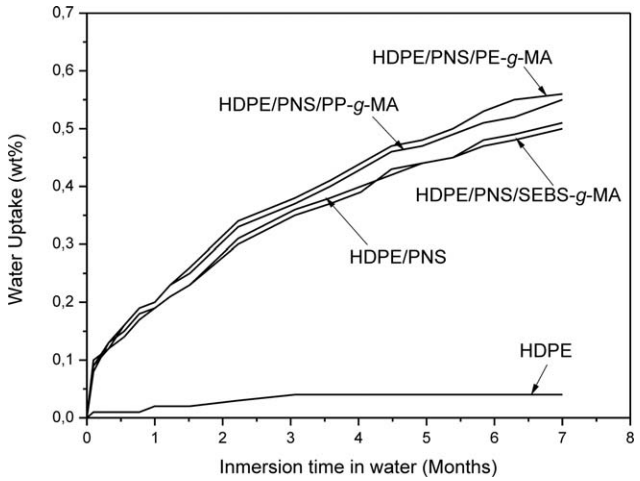

Figure 6. Plot evolution of the water uptake of HDPE/PNS composites (10 wt % PNS) with different compatibilizer agents in terms of the immersion time.

With the aim of evaluating particle dispersion and particle–matrix interface phenomena, a SEM study on fractured surfaces from impact tests was carried out. Figure 4(a) shows a rough surface corresponding to fractured surface of HDPE in impact conditions. Figure 4(b–e) show fractured surfaces from impact tests corresponding to HDPE/PNS composites and quite good particle dispersion can be detected in a rough surface. Addition of highly hydrophilic PNS particles into a highly hydrophobic polyethylene matrix without compatibilizers leads to lack of continuity in HDPE/PNS composites and this is reflected by a remarkable decrease in elongation at break and impact energy. Particle–matrix interactions due to the action of the compatibilizer agents can be observed. In the case of uncompatibilized HDPE/PNS composite [Figure 4(b)] a small gap between the particle and the surrounding matrix can be distinguished. In the case of HDPE/PNS composites compatibilized with PE-*g*-MA [Figure 4(c)] and SEBS-*g*-MA [Figure 4(e)] it is possible to observe persistence of a small gap between the continuous phase (polymer matrix) and the dispersed phase (PNS particles) thus indicating that although some interaction is achieved this is not enough and particle–matrix discontinuity still occurs. That is why cohesion properties such elongation at break and tensile strength are reduced. In these cases, presence of small gaps between particle and matrix confirm that particles act as stress concentrators and this fact leads to fracture with relative small elongation. Nevertheless, HDPE/PNS composites compatibilized with PP-*g*-MA [Figure 4(d)] offer better particle–matrix continuity and this has a positive effect on particle–matrix interactions and this is also reflected in better mechanical properties.

Figure 5 shows the plot evolution of the storage modulus (G') for HDPE and HDPE/PNS composites with different compatibilizing systems. As expected, G' decreases with temperature duo to an increase in chain mobility as temperatures raises up to melt temperature and this is responsible for material softening. Addition of 10 wt % leads to an increase in storage modulus thus indicating a stiffer material; this is due to the fact that PNS particles are stiffer than HDPE polymer chains. In addition, the lack of total continuity leads to low cohesion, which promotes fracture with low deformation levels. If we take into account that a modulus relates the applied stress with the deformation in the elastic region, it is evident that a decrease in deformation leads to higher values for modulus. By comparing the behavior at room temperature as a reference temperature, the storage modulus of PP-*g*-MA compatibilized HDPE/PNS composite (HDPE/PNS/PP-*g*-MA) increases a percentage value of 37% with regard to unfilled HDPE and 26% more than HDPE/PNS composite without compatibilizer.

Figure 6 shows the evolution of the water uptake (percentage increase) of HDPE/PNS composites compared with unfilled HDPE for a period of 7 months. As it can be seen, presence of PNS leads to increased water uptake values with regard to the unfilled HDPE with almost no water uptake due to its extremely high hydrophobicity. All HDPE/PNS composites show similar behavior in terms of the water uptake but PE-*g*-MA compatibilized HDPE/PNS composite (HDPE/PNS/PE-*g*-MA) shows the maximum water uptake in the tested period. Unfilled HDPE shows a water uptake of about 0.04% after 7 months

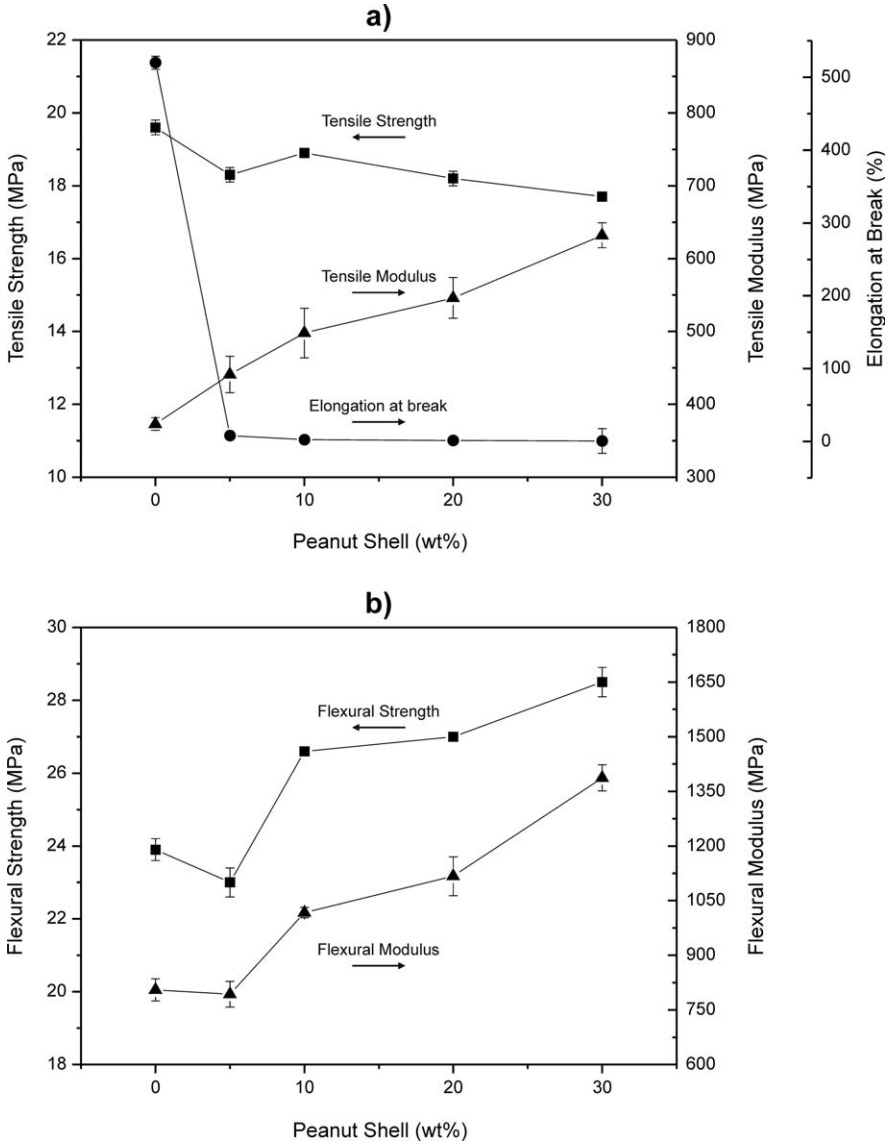

Figure 7. Plot evolution of (a) tensile properties and (b) flexural properties of HDPE/PNS/PP-*g*-MA composites with different filler loads.

and PE-*g*-MA compatibilized offers a water uptake of about 0.56% for the same period and similar values are obtained for all other compatibilized composites. As described by Klyosov[40] typical values of water uptake for Wood Plastic Composites (WPC) with 40–60 wt % wood component, are in the 18–22% range. The values obtained for HDPE composites with 10 wt % PNS are remarkably lower. This is due to the relative low content of lignocellulosic filler (only 10 wt %) but these values are interesting.

By taking into consideration the overall properties obtained with the different maleic anhydride-based compatibilizers, it is possible to conclude that best compatibilizing properties are obtained with PP-*g*-MA (HDPE/PNS/PP-*g*-MA). Although all three compatibilizers offer similar chemical structure, it seems that the maleic anhydride grafting degree is the main parameter related to compatibilization and governs its effectiveness. As indicated in Table II, the PP-*g*-MA copolymer is characterized by a maleic anhydride content of 8–10 wt % which is remarkably higher than the values corresponding to PE-*g*-MA and SEBS-*g*-MA (0.5 and 2 wt %, respectively).

The Effect of PNS Flour Content of HDPE/PNS/PP-*g*-MA Composites

In this section, the effect of the filler content on overall performance of HDPE/PNS/PP-*g*-MA composites is described. Figure 7 shows the plot evolution of mechanical properties (tensile and flexural) of HDPE/PNS/PP-*g*-MA composites with varying amounts of PNS powder.

As we can see, addition of the lignocellulosic filler leads to a slight decrease in tensile strength regarding neat HDPE. The maximum is reached for the composite HDPE/PNS/PP-*g*-MA with 10 wt % PNS with values of about 18.9 MPa. In general, the variability of tensile strength occurs in a very narrow range so that indicating that tensile strength is not practically affected by the filler amount. Variability could be related to typical heterogeneity of polymer–filled materials, so that, maximum and

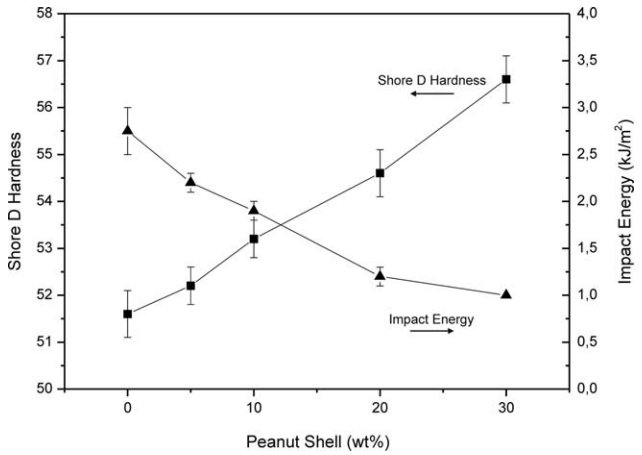

Figure 8. Plot evolution of Shore D hardness and impact energy (Charpy test) for HDPE/PNS/PP-*g*-MA composites in terms of the PNS powder content.

minimum values are not indicative of a tendency. With regard to the Young's modulus it is possible to observe a clear increasing tendency with increasing PNS load. Thus, the modulus of neat HDPE, 373 MPa increases to 632 MPa for the HDPE/PNS/PP-*g*-MA composite containing 30 wt % PNS which represents a percentage increase close to 69%. Nevertheless, as expected, the elongation at break is dramatically reduced after filler addition. As the filler load increases, the elongation at break values change from 520% (unfilled HDPE) up to values of about 0.7% for HDPE/PNS/PP-*g*-MA composites with 30 wt % PNS. This behavior is typical of polymer-filled materials due to the stress concentration phenomena promoted by the presence of dispersed rigid, non-compatible lignocellulosic particles in a highly hydrophobic matrix. With regard to the flexural properties, a clear increasing tendency in both flexural strength and modulus can be observed. The maximum is obtained for a PNS content of 30 wt %. Flexural strength changes from 23 MPa (unfilled HDPE) up to 28.5 MPa for composites containing 30 wt % PNS which represents a percentage increase of about 24%. In the case of the flexural modulus the initial value for unfilled HDPE, 805 MPa, is increased by 72% up to values of about 1387 MPa. Once again, the results give evidence of the negative effect of particle fillers on cohesive properties of polymer composites.

In addition to tensile and flexural properties, Shore D hardness and impact-absorbed energy (Charpy test) were determined for HDPE/PNS/PP-*g*-MA composites with different PNS powder content (Figure 8). As expected, the impact-absorbed energy decreases with the filler content with a minimum value (1 kJ/m^2) for the composite with the highest filler content (30 wt %) which is remarkably lower to the value for unfilled HDPE (2.75 kJ/m^2). As previously indicated, impact energy is directly related to the ability of the material to absorb energy during deformation and fracture; nevertheless, as the deformation capacity of HDPE/PNS/PP-*g*-MA composites is dramatically restricted, then the impact energy is identically reduced. With regard to Shore D hardness, it follows similar tendency to that observed for other mechanical resistant properties. It increases up to 10% higher values for HDPE/PNS/PP-*g*-MA composite with 30 wt % PNS with regard to the unfilled HDPE. In general, the evolution of these two parameters is in total accordance with previous tensile and flexural properties. As the impact-absorbed energy is related to the deformation ability, it follows similar tendency as observed for elongation at break and typical mechanical ductile properties. On the other hand, Shore D hardness is representative for a mechanical resistance property so that, it follows similar tendency as those observed for both tensile and flexural modulus.

The effect of the filler content on melting and thermo-oxidative degradation at moderate temperatures of HDPE/PNS/PP-*g*-MA composites was followed by DSC. Figure 9 shows the plot evolution of melt peak temperatures and thermo-oxidative degradation onset values for HDPE/PNS/PP-*g*-MA composites containing different amounts of PNS powder, obtained by DSC. The melt temperature is slightly lower as the filler content increases changing from 137.4 °C (unfilled HDPE) up to 133.0 °C (HDPE/PNS/PP-*g*-MA composite with 30 wt % PNS). This slight change is related to a slight change in the peak shape but the overall variations in the main parameters related to the melt process are not significant. With regard to the degradation onset temperature at moderate temperatures (thermo-oxidative degradation) we observe a clear increase from 232.5 °C (unfilled HDPE) up to 256.6 °C (HDPE/PNS/PP-*g*-MA composite with 30 wt % PNS). This additional functionality is related to the antioxidant capacity of some components in the lignocellulosic waste, which act as free-radical scavengers thus leading to improved thermal stability at moderate temperatures.

Degradation/decomposition at high temperatures was followed by TGA by measuring the weight loss in function of increasing temperature. TGA curves, as well as the main parameters of the degradation/decomposition process of neat HDPE and HDPE/PNS/PP-*g*-MA composites, are gathered in Figure 10 and Table IV, respectively.

Degradation at high temperatures occurs in two main stages as described previously for composites containing 10 wt % PNS.

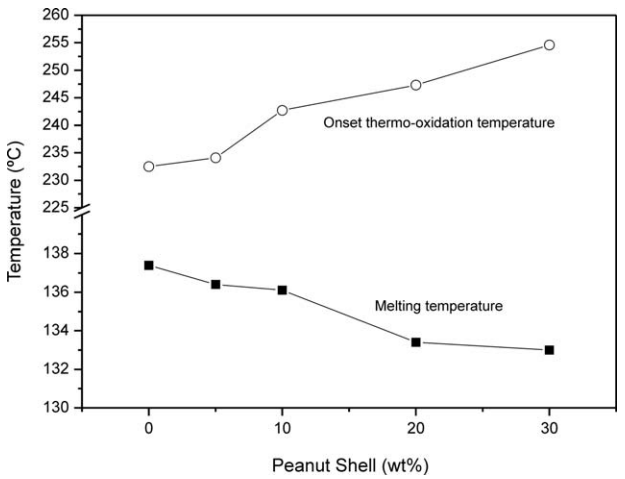

Figure 9. Plot evolution of the thermal properties (melt peak and thermo-oxidation onset temperatures) for HDPE/PNS/PP-*g*-MA composites with different PNS powder content obtained by DSC.

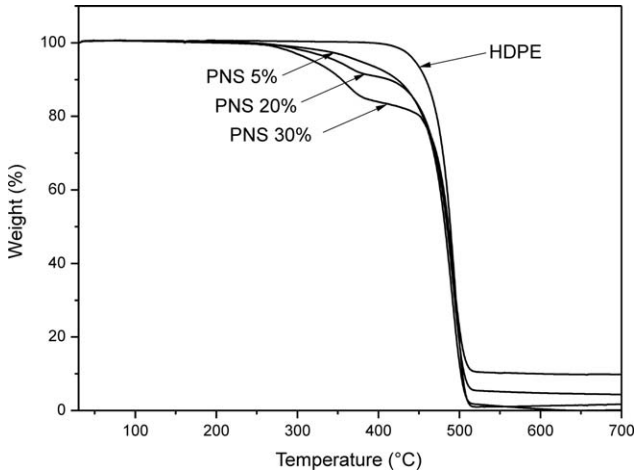

Figure 10. Thermogravimetric curves (TGA) of HDPE/PNS/PP-*g*-MA composites with different PNS powder content.

The addition of PNS powder leads to a decrease in thermal stability of HDPE. This decrease is much higher as the PNS content increases. As it can be seen in Table IV, the onset degradation temperature (T_0) diminishes from 430 °C (neat HDPE) up to values of 287.3 °C for a HDPE/PNS/PP-*g*-MA composite with 30 wt % PNS which represents a percentage decrease of almost 33%. This decrease corresponds to the degradation start of the lignocellulosic component.[41] With regard to the temperature corresponding to the first degradation stage ($T_{max\ 1st}$), it follows similar tendency so that, as the PNS content increases, a slight decrease in this characteristic temperature can be distinguished. Regarding the characteristic degradation temperature of the second stage ($T_{max\ 2nd}$), it does not change in a remarkable way with values around 490 °C for all compositions. In Figure 10 it is possible to observe that as the filler load increases, the step corresponding to PNS degradation increases proportionally and also the residual char increases with PNS content.

The morphology of fractured surface from impact tests of HDPE/PNS/PP-*g*-MA composites with different PNS loading was studied by SEM analysis in order to evaluate the dispersion level and filler–matrix interactions (Figure 11). Figure 11(a) corresponds to fracture of unfilled HDPE and it is characterized by a rough surface. As the filler loading increases, a rough surface with dispersed particles embedded in the matrix [Figure 11(b–e)] can be distinguished. In general, it can be observed quite good

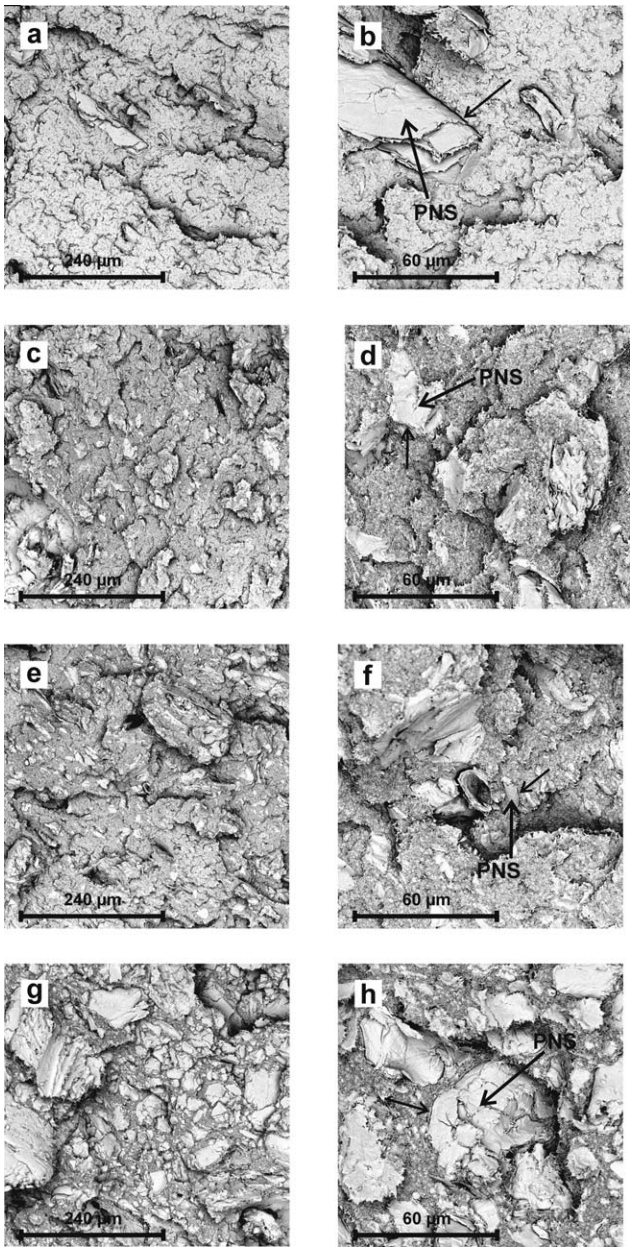

Figure 11. SEM images of fractured surfaces of HDPE/PNS/PP-*g*-MA composites with different PNS powder: (a) 5 w % (500×), (b) 5 wt % (2000×), (c) 10 wt % (500×), (d) 10 wt % (2000×), (e) 20 wt % (500×), (f) 20 wt % (2000×), (g) 30 wt % (500×), and (h) 30 wt % (2000×).

Table IV. Thermal Degradation Parameters of HDPE/PNS/PP-*g*-MA Composites with Different PNS Powder Content Obtained by TGA

wt % PNS	T_0[a] (°C)	$T_{max\ 1st}$ (°C)	$T_{max\ 2nd}$ (°C)
0 (HDPE)	430	—	495.3
5	327.3	—	490.3
10	325.3	364.3	490.3
20	305.0	363.0	491.0
30	287.3	360.6	490.6

[a] T_0, calculated at 5% mass loss.

particle dispersion together with some particle–matrix interactions as the gaps between the particles and the surrounding matrix are small. Nevertheless, the increasing amount of filler leads to a remarkable decrease in ductile properties as evidenced by the evolution of elongation at break and impact energy.

The effect of the filler content was also tested by DMTA in torsion mode. Figure 12 shows a comparative plot of the storage modulus (G') of HDPE/PNS/PP-*g*-MA composites with varying filler content in terms of temperature. As we have described previously with regard to flexural and tensile properties a clear increase in the corresponding modulus occurs with increasing

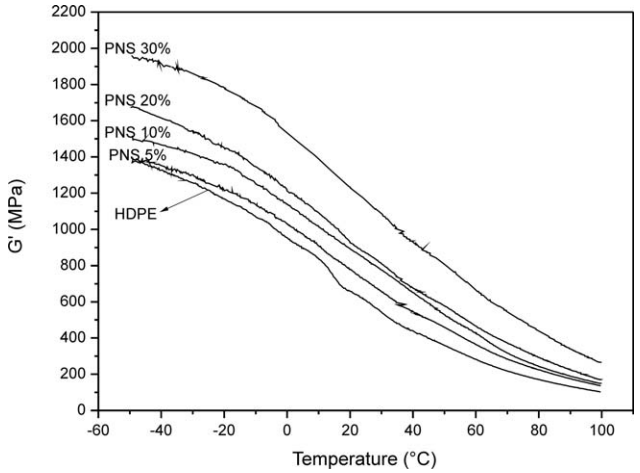

Figure 12. Evolution of the storage modulus (G') of HDPE/PNS/PP-*g*-MA composites with different weight percentages of PNS powder.

filler content. This fact is also observed with the evolution of the storage modulus with temperature for all HDPE/PNS/PP-*g*-MA composites. As the filler load increases, the ability to deform is restricted due to the stress concentration effect provided by the dispersed particles. If we compare the storage modulus values at room temperature, HDPE/PNS/PP-*g*-MA containing 30 wt % offers G' values 92% higher than unfilled HDPE. It is also important to remark that high differences in storage modulus are detected at room temperature but the difference gets lower as temperature increases.

CONCLUSIONS

The main aim of this work was to evaluate the influence of three different maleic anhydride copolymers as compatibilizers for HDPE/PNS composites, namely: polyethylene-*graft*-maleic anhydride (PE-*g*-MA), polypropylene-*graft*-maleic anhydride (PP-*g*-MA), and polystyrene-*block*-poly(ethylene-*ran*-butylene)-*block*-polystyrene-*graft*-maleic anhydride (SEBS-*g*-MA). Although all three compatibilizers have maleic anhydride functionality, the best results were obtained with PP-*g*-MA with a percentage increase in tensile and flexural modulus of about 16% and 26%, respectively, with regard to unfilled HDPE. SEM analysis revealed absence of matrix–particle interaction in uncompatibilized HDPE/PNS composites. Despite this, all three compatibilizers offer some matrix–particle interactions as evidenced by a reduction of the gap size between the dispersed particles and the surrounding polymer matrix.

The addition of 30 wt % PNS led to composite materials with interesting properties from different points of view. In a first approach, flexural strength and modulus increased by 24% and 72%, respectively, but the most interesting property was a remarkable increase in the thermo-oxidative degradation onset temperature which changed from 232 °C (unfilled HDPE) up to 254 °C in composites with 30 wt % PNS. This additional feature was due to the natural intrinsic antioxidant components in PNS (polyphenols and flavonoids) which act as free-radical scavengers thus delaying thermo-oxidative processes.

As a general conclusion it is possible to say that manufacturing of natural fiber reinforced plastics (NFRP) with biobased polyethylene and PNS powder, a by-product of the peanut industry, can be obtained by extrusion-compounding followed by injection molding. These composites offer a clearly positive environmental efficiency together with balanced overall properties.

ACKNOWLEDGMENTS

This research was supported by the Ministry of Economy and Competitiveness -MINECO, Ref: MAT2014-59242-C2-1-R. Authors also thank to "Conselleria d'Educació, Cultura i Esport" - Generalitat Valenciana, Ref: GV/2014/008 for financial support. A. Carbonell-Verdu wants to thank Universitat Politècnica de València for financial support through an FPI grant. D. Garcia-Garcia wants to thanks the Spanish Ministry of Education, Culture and Sports for the financial support through an FPU grant (FPU13/06011).

REFERENCES

1. Zini, E.; Scandola, M. *Polym. Compos.* **2011**, *32*, 1905.
2. Koutsomitopoulou, A. F.; Benezet, J. C.; Bergeret, A.; Papanicolaou, G. C. *Powder Technol.* **2014**, *255*, 10.
3. Ashori, A. *Bioresour. Technol.* **2008**, *99*, 4661.
4. García-García, D.; Carbonell, A.; Samper, M.; García-Sanoguera, D.; Balart, R. *Compos. Part B* **2015**, *78*, 256.
5. Essabir, H.; Nekhlaoui, S.; Malha, M.; Bensalah, M. O.; Arrakhiz, F. Z.; Qaiss, A.; Bouhfid, R. *Mater. Des.* **2013**, *51*, 225.
6. Mohanty, A. K.; Misra, M.; Drzal, L. T. *J. Polym. Environ.* **2002**, *10*, 19.
7. Mohanty, A. K.; Misra, M.; Hinrichsen, G. *Macromol. Mater. Eng.* **2000**, *276*, 1.
8. Shah, D. U. *J. Mater. Sci.* **2013**, *48*, 6083.
9. Balart, J.; Fombuena, V.; Fenollar, O.; Boronat, T.; Sánchez-Nacher, L. *Compos. Part B* **2016**, *86*, 168.
10. Kim, H. S.; Kim, S.; Kim, H. J.; Yang, H. S. *Thermochim. Acta* **2006**, *451*, 181.
11. Poletto, M.; Zattera, A. J.; Santana, R. M. C. *Polym. Compos.* **2014**, *35*, 1935.
12. Salleh, F. M.; Hassan, A.; Yahya, R.; Lafia-Araga, R. A.; Azzahari, A. D.; Nazir, M. N. Z. M. *J. Polym. Res.* **2014**, *21*,
13. Ayrilmis, N.; Kaymakci, A. *Ind. Crops Prod.* **2013**, *43*, 457.
14. Sailaja, R. R. N.; Girija, B. G.; Madras, G.; Balasubramanian, N. *J. Mater. Sci.* **2008**, *43*, 64.
15. Etaati, A.; Pather, S.; Fang, Z.; Wang, H. *Compos. Part B* **2014**, *62*, 19.
16. Petchwattana, N.; Covavisaruch, S.; Chanakul, S. *J. Polym. Res.* **2012**, *19*,
17. Hassanabadi, H. M.; Alemdar, A.; Rodrigue, D. *J. Appl. Polym. Sci.* **2015**, *132*, DOI: 10.1002/app.42438.
18. Danyadi, L.; Moczo, J.; Pukanszky, B. *Compos. Part A* **2010**, *41*, 199.

19. Wilson, K.; Yang, H.; Seo, C. W.; Marshall, W. E. *Bioresour. Technol.* **2006**, *97*, 2266.
20. Bilir, M. H.; Sakalar, N.; Acemioglu, B.; Baran, E.; Alma, M. H. *J. Appl. Polym. Sci.* **2013**, *127*, DOI: 10.1002/app.37614.
21. Rivilli, P. L.; Alarcón, R.; Isasmendi, G. L.; Pérez, J. D. *BioResources* **2011**, *7*, 0112.
22. Sareena, C.; Ramesan, M. T.; Purushothaman, E. *J. Appl. Polym. Sci.* **2012**, *125*, 2322.
23. Wu, C. S. *Polym. Degrad. Stabil.* **2012**, *97*, 2388.
24. Salasinska, K.; Ryszkowska, J. *Polimery* **2013**, *58*, 461.
25. Zaaba, N. F.; Ismail, H.; Jaafar, M. *BioResources* **2014**, *9*, 2128.
26. Prabhakar, M. N.; Shah, A. U. R.; Rao, K. C.; Song, J. I. *Fibers Polym.* **2015**, *16*, 1119.
27. Batalla, L.; Nunez, A. J.; Marcovich, N. E. *J. Appl. Polym. Sci.* **2005**, *97*, 916.
28. Sareena, C.; Ramesan, M. T.; Purushothaman, E. *Polym. Compos.* **2012**, *33*, 1678.
29. Adhikary, K. B.; Pang, S.; Staiger, M. P. *Compos. Part B* **2008**, *39*, 807.
30. Migneault, S.; Koubaa, A.; Perré, P.; Riedl, B. *Appl. Surf. Sci.* **2015**, *343*, 11.
31. Chang, F. C.; Kadla, J. F.; Lam, F. *Eur. J. Wood Wood Prod.* **2016**, *74*, 23.
32. Ferrero, B.; Fombuena, V.; Fenollar, O.; Boronat, T.; Balart, R. *Polym. Compos.* **2015**, *36*, 1378.
33. Sabetzadeh, M.; Bagheri, R.; Masoomi, M. *Carbohydr. Polym.* **2015**, *119*, 126.
34. Liu, H.; Wu, Q.; Zhang, Q. *Bioresour. Technol.* **2009**, *100*, 6088.
35. Farsi, M. *Fibers Polym.* **2012**, *13*, 515.
36. Sewda, K.; Maiti, S. N. *J. Appl. Polym. Sci.* **2009**, *112*, 1826.
37. Lee, S. H.; Wang, S. Q. *Compos. Part A* **2006**, *37*, 80.
38. Bledzki, A. K.; Mamun, A. A.; Volk, J. *Compos. Part a* **2010**, *41*, 480.
39. Ou, R.; Xie, Y.; Wang, Q.; Sui, S.; Wolcott, M. P. *J. Appl. Polym. Sci.* **2014**, *131*, DOI: 10.1002/app.40331.
40. Klyosov, A. A., Wood-Plastic Composites; John Wiley & Sons: New York, **2007**.
41. Petinakis, E.; Liu, X.; Yu, L.; Way, C.; Sangwan, P.; Dean, K.; Bateman, S.; Edward, G. *Polym. Degrad. Stabil.* **2010**, *95*, 1704.